ChemComm

Accepted Manuscript

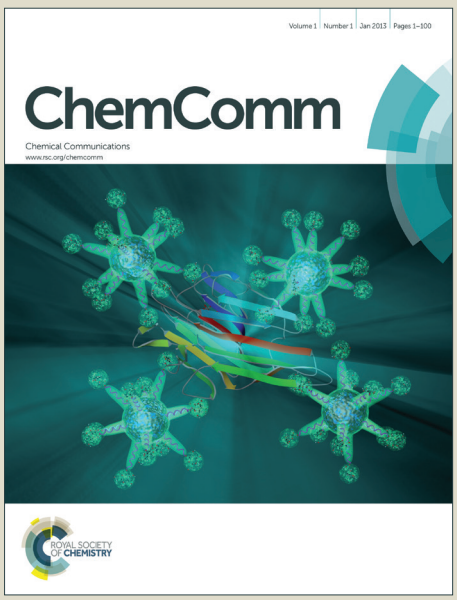

ROYAL SOCIETY OF CHEMISTRY

www.rsc.org/chemcomm

Journal Name

RSCPublishing

COMMUNICATION

High-yield production of highly conductive graphene via reversible covalent chemistry

Cite this: DOI: 10.1039/x0xx00000x

Zhe Ji,[a] Ji Chen[a], Liang Huang[a], Gaoquan Shi[a]*

Received 00th January 2012,
Accepted 00th January 2012

DOI: 10.1039/x0xx00000x

www.rsc.org/

On the basis of the Diels-Alder reaction of graphite and tetracyanoethylene, graphite has been mechanically exfoliated into graphene adducts in a yield up to 38%. The graphene adduct can restore its conjugated structure via retro-Diels-Alder reaction under mild conditions, exhibiting a high conductivity of 1035 S m^{-1}.

Graphene has recently intrigued intense research effort because of its atom-thick two-dimensional structure, and remarkable electrical and thermal conductivities, high mechanical strength and huge specific surface area.[1] The unique structure and superior physical properties render graphene potential applications in field-effect transistor, ultracapacitor, transparent conducting film, catalysis and sensor.[2] However, these applications are practically impeded by the difficulty in the high-yield production of high-quality graphene. Fortunately, nature provides us with a cheap and easily available graphene resource: graphite, composing of stacked graphene layers. Although mechanical exfoliation of graphite with Scotch tape led to the discovery of graphene,[3] the production of graphene via wet chemical approaches is more scalable and processable. To exfoliate graphite into few-layer graphene sheets, strong interaction between solvent molecules and graphene sheets is required. Using N-methylpyrrolidone (NMP) as the solvent, Coleman et al. developed a graphene production method based on sonication-assisted liquid-phase exfoliation.[4] Unfortunately, this strategy usually has a low conversion yield.

The widely used technique for the high-yield production of chemically converted graphene is Hummers' method.[5] It involves harsh oxidation and covalent modification of graphite with oxygen-containing groups.[6] These hydrophilic groups increase the interlayer distance and provide strong electrostatic repulsion between graphene sheets, leading to intrinsically facile exfoliation and stabilization of single-layer graphene oxide (GO) sheets in water.[7] However, oxygen-containing groups heavily destroy the conjugated basal planes of graphene sheets; thus GO is actually an insulator. The conjugated structure and conductivity of GO can be partially recovered by chemical, thermal or light-assisted reduction;[8] however, a considerable amount of defects and oxygenated groups still remain in reduced GO (rGO). Up to date, a technique that can completely restore the conjugated sp^2 carbon network of chemically converted graphene in liquid media has not yet been developed.

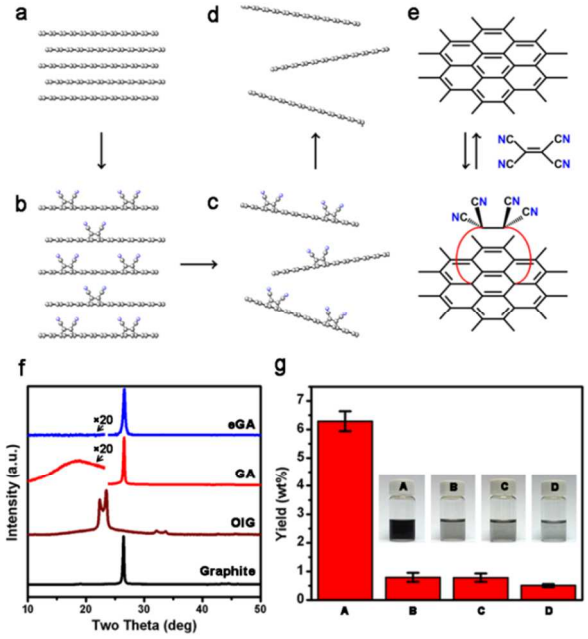

Fig. 1. A reversible covalent chemistry route to the production of graphene. (a) Graphite, (b) graphite adduct with TCNE addends covalently bound on graphene basal planes after Diels-Alder reaction, (c) sonication-exfoliated GA dispersed in NMP, (d) eGA dispersion with sp^2 network restored by the retro-Diels-Alder reaction. (e) Reaction scheme of the reversible Diels-Alder reaction between graphene and TCNE. (f) XRD patterns of graphite, OIG, thin films of GA and eGA. The XRD patterns of GA and eGA in the region below 23.5° have been magnified by a factor of 20 for clarity. (g) Histograms of the yields of (A) GA from the graphite treated by oleum and TCNE, (B) graphene from the graphite treated by oleum, (C) graphene from the graphite treated by TCNE and (D) graphene from pristine graphite; the error bars indicate the statistical variations. Inset: photographs of the exfoliated GA or graphene dispersions.

Recently, Haddon and co-workers reported that graphene can be used as either a diene or a dienophile for reversible Diels-Alder reactions because of its zero band gap electronic structure.[9] The Diels-Alder reactivity of graphite has also been proposed and proved to be effective for producing dispersible graphene nanoplatelets.[10] However, reversible covalent chemistry has never been explored for the mass-production of graphene, albeit this strategy combines the advantage of covalent chemistry for effective exfoliation of graphite and that of non-covalent chemistry for preserving the conjugated π-system of graphene. Herein, we report a high-yield wet chemical method to produce highly conductive graphene via a reversible Diels-Alder reaction. In this case, the covalently bound tetracyanoethylene (TCNE) moieties on graphene sheets enable the mechanical exfoliation of graphite into dispersible graphene adducts (GA). The temporarily disrupted π-system of GAs can be restored after retro-Diels-Alder reaction under a mild condition in liquid media and the resultant eliminated GA (eGA) exhibits a high conductivity comparable to that of pristine graphene.

The procedure of high-yield production of graphene via the reversible covalent chemistry is depicted in **Fig. 1.** Diels-Alder reaction was used to bond TCNE molecules onto the graphene layers of graphite to weaken the interlayer interactions and to improve the dispersibility of resulting graphene sheets. To increase the efficiency of Diels-Alder reaction, graphite was firstly treated with oleum into oleum-intercalated graphite (OIG, **a**) because of the following reasons: (1) oleum intercalation expands graphite basal spacing, opening the avenues for the penetration of TCNE molecules into the graphite crystals; (2) as a Lewis acid, oleum can function as a catalyst for Diels-Alder reaction; (3) mild oxidation caused by oleum[11] activates graphite to provide sufficient sp^3 carbons for Diels-Alder reaction, because computations predicted that the basal plane of pristine graphene is nearly inert to Diels-Alder reaction while defects and edges are much more active.[12] After Diels-Alder reaction, graphite-TCNE adduct (**b**) was exfoliated by ultrasonication to form a stable dispersion of GA (**c**) in NMP. The GA dispersion was then subjected to heating at 100 °C for 3 h to perform retro-Diels-Alder reaction. The cleavage and removal of TCNE addends from GA led to the formation of high-quality eGA sheets dispersible in NMP (**d**). The scheme of reversible Diels-Alder reaction on a graphene sheet is shown in (**e**).

The process of producing high-quality graphene was traced by comparing the interlayer distances of graphite, OIG, GA and eGA (**Fig. 1f**). The X-ray diffraction (XRD) pattern of graphite shows a strong and sharp peak at 26.5°, corresponding to an expected basal spacing of 0.335 nm. The pattern of OIG has [002] diffraction lines centred at 22° along with [003] lines around 33°.[13] Accordingly, the basal spacing of [001] lattice planes was calculated to be 0.800 nm, indicating the formation of intercalated compounds. The XRD pattern of GA film exhibits a new broad and weak peak at 19°. This peak is attributed to the expansion of layer-to-layer distance of graphite caused by TCNE addends covalently bound to the basal planes of graphene sheets. When TCNE addends were removed upon retro-Diels-Alder reaction, the diffraction line at 19° disappeared and only a sharp peak related to pristine graphene sheets stacking along their *c*-axis was observed.

With the assistances of expanded interlayer distances and improved solvent affinity, the graphite flakes treated by oleum and TCNE can be mechanically exfoliated into GA sheets to form a stable dispersion in NMP. To demonstrate the efficiency of our reversible covalent strategy, we compared this system to that without TCNE treatment or without oleum intercalation, or without both. A deep black dispersion of GA was obtained after sonication of TCNE-graphite adducts for 1 h and successively purified by centrifugation

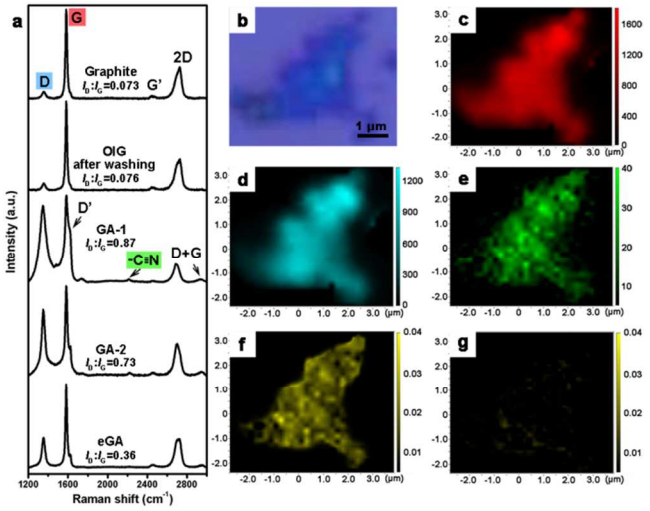

Fig. 2. The reaction sequence monitored by Raman spectroscopy. (a) Raman spectra of graphite, OIG, individual GA and eGA sheets with a normalized intensity of G-bands. OIG sample was washed by water before Raman measurement to avoid the intervention of intercalating oleum. (b) Microscopic image of a GA-2 sheet on a 300 nm-thick SiO_2 coated Si wafer. (c–g) The corresponding Raman mapping of GA-2 for G- (c), D- (d) and cyano-bands (e), the intensity ratio of cyano-band to G-band before (f) and after (g) retro-Diels-Alder reaction.

(**Fig. 1g**, inset). In the control systems, only light grey dispersions were obtained through the same preparation and purification processes. The concentration of GA dispersion was measured by UV-visible spectroscopy (**Fig. S1,** ESI†). The yield of GA was calculated to be 6.3 wt% (mass ratio of GA over feeding graphite) based on Lambert-Beer law (**Fig. 1g**). In comparison, the yields of the graphene produced in control systems were nearly 10 times lower. The yield of GA can be increased by the recycling use of the sediment obtained by centrifugation. After each cycle, newly generated defects and edge sites were exposed for Diels-Alder reaction in the successive cycle to guarantee the continuing exfoliation. After 10 cycles, an overall yield of 38 wt% was achieved. Accordingly, the yield of this reversible covalent strategy is comparable to that of conventional oxidation method.[14]

The GA sheets are morphologically similar to that of the graphene sheets prepared by conventional liquid phase exfoliation of graphite. The typical transmission electron microscope (TEM) images (**Fig. S2,** ESI†) show that these GA sheets have lateral dimensions ranging from hundreds of nanometers to several micrometers. About 60% of the eGA flakes are thinner than five layers of graphene and have an average lateral dimension of 0.4 μm according to their atomic force microscope (AFM) images (**Fig. S3,** ESI†) and scanning electron micrographs (SEM) (**Fig. S4**, ESI†).

To confirm the reversible disruption and recovery of conjugation system of GA flakes, Raman spectroscopy was employed to characterize the chemical structures of individual GA or eGA flakes. As shown in **Fig. 2a**, pristine graphite powder exhibits a sharp and strong G-band at 1580 cm^{-1} associated with the E_{2g} mode of graphite or graphene.[15] A weak band at 1350 cm^{-1} is assigned to the D-band of carbon materials. Because D-band does not exist in defect-free graphite, its intensity is an indication of the degree of defects and edges in graphitic materials. Compared with the starting graphite, OIG shows a slight increase in the intensity ratio of D- to G-band (I_D:I_G) from 0.073 to 0.076, indicating the mild oxidation by oleum. Diels-Alder cycloaddition reaction generated abundant sp^3 carbon

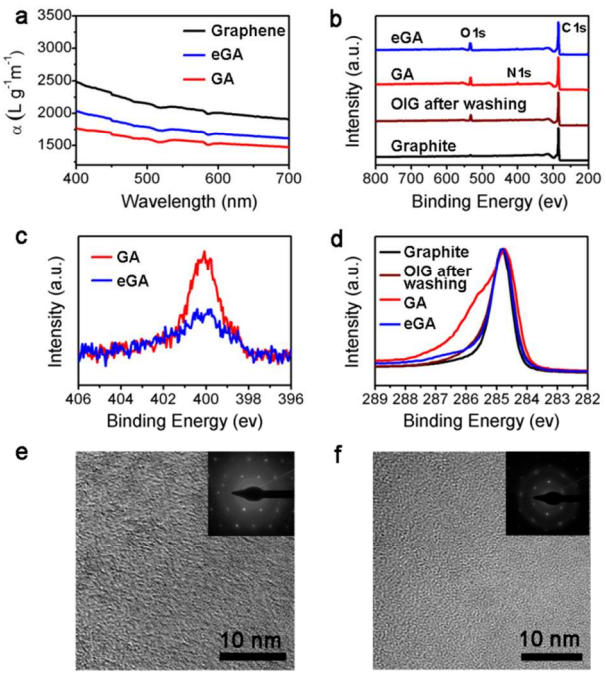

Fig. 3. (a) Absorption spectra of graphene, eGA and GA dispersions; solvent: NMP. (b) XPS survey spectra of graphite, OIG, GA and eGA with normalized C1s peaks. (c) N1s XPS spectra of GA and eGA. (d) C1s XPS spectra of graphite, OIG, GA and eGA. OIG sample was washed by water before XPS measurement to avoid the intervention of intercalating oleum. (e, f) HRTEM image and ED pattern of a GA (e) or an eGA (f) flake.

atoms on exfoliated GA sheets, giving an I_D:I_G as high as 0.87 for a severely adducted graphene (GA-1) or 0.73 for a typically adducted graphene (GA-2). The weak band at 2210 cm^{-1} is assigned to the stretching of cyano groups from TCNE addends,[9] further confirming the formation of GA by Diels-Alder reaction. Furthermore, the distribution of functional groups on GA flakes was studied by Raman mapping. The optical microscope image of a GA-2 flake and its Raman intensity mappings for G-, D- and the cyano stretching vibration bands are demonstrated in **Fig. 2b** to **Fig. 2e,** respectively. Accordingly, the distributions of functional groups on a GA flake are similar to that of the randomly distributed oxidized domains of a GO sheet.[15] The intensity of cyano stretching vibration band has been normalized with respect to that of G-band and its specific intensity (I_{cyano}:I_G) is shown in **Fig. 2f**. The I_{cyano}:I_G mapping shows scattered spots, indicating that TCNE addends are clustered on the basal plane of GA flake. This distribution pattern makes sense since the Diels-Alder reaction is more favorable to occur at defective domains. The carbon atoms connected with TCNE addends by sp^3 bonds, leading their surrounding C=C double bonds to be active for successive Diels-Alder reaction. Thus, the original tiny defects can be extended into clusters by TCNE addends.

Raman spectroscopy was also used to monitor the retro-Diels-Alder reaction. After soaking a silica chip of GA-2 in the NMP dispersion at 100 °C for 3 h followed by repeated washing with ethanol, the resulting eGA flake exhibited a Raman spectrum typical for pristine multilayer graphene. The absence of 2210 cm^{-1} band both in the spectrum (**Fig. 2a**) and in the mapping (**Fig. 2g**) reflects the cleavage of TCNE addends after mild heating. The elimination of TCNE addends also weakened the intensity of D-band and the I_D:I_G ratio decreased to 0.36, indicating a partial restoration of conjugated structure.

The restoration of conjugated structure of GA by retro-Diels-Alder reaction has also been confirmed by other techniques. As shown in **Fig. 3a**, the disrupted conjugation network of GA led to its optical absorbance coefficient smaller than that of pristine graphene. After retro-Diels-Alder reaction, eGA exhibited a partially restored absorbance. The X-ray photoelectron spectra (XPS) survey curve of pristine graphite exhibits only a pronounced C1s peak at 284.5 eV (**Fig. 3b**). The curve of OIG shows a weak O1s peak (~532 eV) caused by mild oxidation. After Diels-Alder reaction, a new weak peak (~400 eV) corresponding to N1s was observed for GA. Its C:N atomic ratio was calculated to be 26.8, indicating that about every 91 graphitic carbon atoms were adducted by one TCNE molecule. The cleavage of TCNE addends is reflected by the much weaker N1s XPS peak of eGA than that of GA (**Fig. 3c**). The N1s signal of eGA is possibly attributed to the residual TCNE attends and NMP molecules. High-resolution C1s XPS spectra were employed to identify the chemistry states of carbon atoms. According to **Fig. 3d**, the peak of OIG has a slight deviation from that of graphite at ~286 eV, indicating the existence of C-O species. The spectrum of GA exhibits a broad shoulder in the range of 285–288 eV, relating to the TCNE-graphene adducts. As expected, after retro-Diels-Alder reaction, eGA exhibits a C1s peak similar to that of pristine graphite, confirming the formation of more perfect graphene basal planes. The functionalization and restoration of graphene basal plane have also been confirmed by high-resolution TEM (HRTEM) images shown in **Fig. 3e** and **3f**. The surface of a GA flake was covered by amorphous TCNE addends according to its blurred HRTEM image (**Fig. 3e**). Its electron diffraction (ED) exhibits a hexagonal pattern corresponding to the retained carbon lattices. On the contrary, eGA shows a HRTEM identical to that of a pristine monolayer graphene with a shaper ED pattern (**Fig. 3f**). Taken altogether, the disrupted conjugation network was restored by retro-Diels-Alder reaction to give high quality graphene.

To achieve better insight into the high-quality of eGA, we fabricated eGA thin films and measured their conductivities as a proof-of-concept application. These films were prepared by vacuum filtration of graphene dispersions followed by vacuum drying at room temperature for 12 h. The resistance of the film was plotted versus the reciprocal of its thickness calculated from the mass of graphene in the dispersion (**Fig. S5,** ESI†). The linear plots gave the conductivities of GA, eGA and conventionally exfoliated graphene to be 135, 1035, and 1672 S m^{-1} respectively. The retro-Diels-Alder reaction resulted in a pronounced increase in conductivity due to the restored conjugation network in eGA. The conductivity of eGA is comparable to the graphene prepared by conventional liquid-phase exfoliation.[4] This value is several magnitudes higher than that of GO, even though no annealing or other post-treatment was performed. The slightly lower conductivity of eGA than that of the conventionally exfoliated graphene is possibly caused by the structural defects and a trace amount of residual TCNE addends on eGA sheets.

Conclusions

We developed a reversible covalent strategy for the high-yield production of few-layer graphene. This technique can exfoliate graphite into GA via a Diels-Alder reaction with a yield up to 38%. The exfoliated GA can restore its π-system by retro-Diels-Alder reaction under a mild condition. All reactions and exfoliation were performed in liquid phase, compatible with various material processing processes. The resultant eGA exhibits a high conductivity of 1035 S m^{-1} without annealing, which is comparable to pristine graphene prepared by

conventional liquid-phase exfoliation. The high yield of producing high-quality graphene is important for commercial applications of this material. This process is very clean because no byproduct is produced. It even has the potential to maximize its atom economy by the recycling use of TCNE molecules eliminated from GA upon retro-Diels-Alder reaction.

This work was supported by the National Basic Research Program of China (973 Program, 2012CB933402, 2013CB933001), Natural Science Foundation of China (51161120361, 51433005), and Research Grant of Incheon National University in 2014.

Notes and references

[a] Department of Chemistry, Tsinghua University, Beijing 100084, People's Republic of China. Email: gshi@tsinghua.edu.cn

† Electronic Supplementary Information (ESI) available: Experimental section and supplementary figures. See DOI: 10.1039/c000000x/

1 M. J. Allen, V. C.Tung, R. B. Kaner, *Chem. Rev*., 2009, **110**, 132; D. R. Dreyer, R. S. Ruoff, C. W. Bielawski, *Angew. Chem. Inter. Ed*., 2010, **49**, 9336; A. K. Geim, *Science*, 2009, **324**, 1530; K. S. Novoselov, V. Fal, L. Colombo, P. Gellert, M. Schwab, K. Kim, *Nature*, 2012, **490**, 192; H. Bai, C. Li, X. L. Wang, G. Q. Shi, *Chem. Commun.,* 2010, **46**, 2376; Y. Zhu, S. Murali, W. Cai, X. Li, J. W. Suk, J. R. Potts, R. S. Ruoff, *Adv. Mater.,* 2010, **22**, 3906.

2 A. A. Balandin, *Nat. Mater.*, 2011, **10**, 569; C. Lee, X. Wei, J. W. Kysar, J. Hone, *Science*, 2008, **321**, 385; M. D. Stoller, S. Park, Y. Zhu, J. An, R. S. Ruoff, *Nano Lett.*, 2008, **8**, 3498; Q. Wu, Y. X. Xu, Z. Y. Yao, A, R. Liu, G. Q. Shi, *ACS Nano*, 2010, **4**, 1963; H. Bai, Y. X. Xu, L. Zhao, C. Li, G. Q. Shi, *Chem. Commun.,* 2009, 1667; T. X. Wei, Y. Y. Chen, W. W. Tu, Y. Q. Lan, Z. H. Dai, *Chem. Commun.,* 2014, **50**, 9357.

3 K. S. Novoselov, A. K. Geim, S. Morozov, D. Jiang, Y. Zhang, S. Dubonos, I. Grigorieva, A. Firsov, *Science*, 2004, **306**, 666.

4 Y. Hernandez, V. Nicolosi, M. Lotya, F. M. Blighe, Z. Sun, S. De, I. McGovern, B. Holland, M. Byrne, Y. K. Gun'Ko, J. J. Boland, P. Niraj, G. Duesberg, S. Krishnamurthy, R. Goodhue, J. Hutchison, V. Scardaci, A. C. Ferrari, J. N. Coleman, *Nat. Nanotechnol.*, 2008, **3**, 563.

5 W. S. Hummers Jr., R. E. Offeman, *J. Am. Chem. Soc.*, 1958, ***80***, 1339.

6 A. Lerf, H. He, M. Forster, J. Klinowski, *J. Phys. Chem. B*, 1998, **102**, 4477; W. Cai, R. D. Piner, F. J. Stadermann, S. Park, M. A. Shaibat, Y. Ishii, D. Yang, A. Velamakanni, S. J. An, M. Stoller, *Science*, 2008, **321**, 1815.

7 S. Stankovich, R. D. Piner, X. Chen, N. Wu, S. T. Nguyen, R. S. Ruoff, *J. Mater. Chem.*, 2006, **16**, 155.

8 S. Stankovich, D. A. Dikin, R. D. Piner, K. A. Kohlhaas, A. Kleinhammes, Y. Jia, Y. Wu, S. T. Nguyen, R. S. Ruoff, *Carbon*, 2007, **45**, 1558; V. C. Tung, M. J. Allen, Y. Yang, R. B. Kaner, *Nat. Nanotechnol.*, 2009, **4**, 25; H. C. Schniepp, J.-L. Li, M. J. McAllister, H. Sai, M. Herrera-Alonso, D. H. Adamson, R. K. Prud'homme, R. Car, D. A. Saville, I. A. Aksay, *J. Phys. Chem. B*, 2006, **110**, 8535; G. Williams, B. Seger, P. V. Kamat, *ACS Nano*, 2008, **2**, 1487.

9 S. Sarkar, E. Bekyarova, S. Niyogi, R. C. Haddon, *J. Am. Chem. Soc.*, 2011, **133**, 3324.

10 T. M. Swager, *ACS Macro Lett.*, 2011, **1**, 3; J.-M. Seo, I.-Y. Jeon, J.-B. Baek, *Chem. Sci.*, 2013, **4**, 4273.

11 X. Li, G. Zhang, X. Bai, X. Sun, X. Wang, E. Wang, H. Dai, *Nat. Nanotechnol.*, 2008, **3**, 538.

12 P. A. Denis, *Chem. Eur. J.*, 2013, **19**, 15719; Y. Cao, S. Osuna, Y. Liang, R. C. Haddon, K. Houk, *J. Am. Chem. Soc.*, 2013, **135**, 17643.

13 B.-J. Lee, *Bull. Korean Chem. Soc.*, 2002, **23**, 1801.

14 J. Chen, B. Yao, C. Li, G. Shi, *Carbon*, 2013, **64**, 225.

15 A. Ferrari, J. Meyer, V. Scardaci, C. Casiraghi, M. Lazzeri, F. Mauri, S. Piscanec, D. Jiang, K. Novoselov, S. Roth, *Phys. Rev. Lett.*, 2006, **97**, 187401.

